Direct Myocardial Strain Assessment from Frequency Estimation in Tagging MRI

H.B. Kause[1], O.G. Filatova[1], R. Duits[2,3], L.C.M. Bruurmijn[2], A. Fuster[2,3], J.J.M. Westenberg[4], L.M.J. Florack[2,3], and H.C. van Assen[1]

[1] Department of Electrical Engineering
[2] Department of Biomedical Engineering
[3] Department of Mathematics & Computer Science
Eindhoven University of Technology, The Netherlands (www.iste.nl)
[4] Department of Radiology, Leiden University Medical Center, The Netherlands

Abstract. We propose a new method to analyse deformation of the cardiac left ventricular wall from tagging magnetic resonance images. The method exploits the fact that the time-dependent frequency covector field representing the tag pattern is tightly coupled to the myocardial deformation and not affected by tag fading. Deformation and strain tensor fields can be retrieved from local frequency estimates given at least n (independent) tagging sequences, where n denotes spatial dimension. Our method does not require knowledge of material motion or tag line extraction. We consider the conventional case of two tag directions, as well as the overdetermined case of four tag directions, which improves robustness. Additional scan time can be prevented by using one or two grid patterns consisting of multiple, simultaneously acquired tag directions. This concept is demonstrated on patient data. Tracking errors obtained for phantom data are smaller than those obtained by HARP, 0.32 ± 0.14 px versus 0.53 ± 0.07 px. Strain results for volunteers are compared with corresponding linearised strain fields derived from HARP.

Keywords: Tagging Magnetic Resonance Imaging, Myocardial Deformation, Myocardial Strain, Gabor Transform, Frequency Analysis

1 Introduction

Cardiovascular disease (CVD) is globally the leading cause of death[1] with estimated 17.3 million deaths in 2008 (30% of all global deaths). Therefore it is important to develop methods for diagnosis and therapy assessment at early stages of the disease. In literature it has been reported that heart disease may affect *strain* before remodelling occurs as a consequence of persistent heart dysfunction [1, 2].

[1] World Health Organization, Fact sheet N° 317, September 2012.

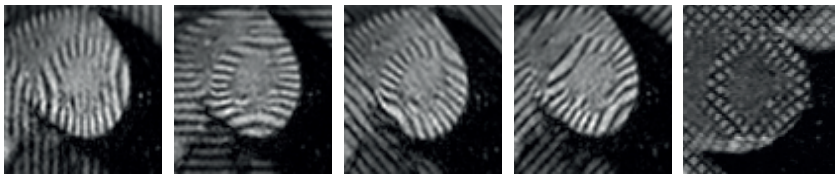

Fig. 1. Short-axis tMRI images of a left ventricle in systole.

Speckle tracking echocardiography [3] is often the initial choice for cardiac movement assessment, since it is relatively cheap and widely accessible. However, the estimated strain depends on the angle of imaging and therefore the results are highly operator sensitive. In order to avoid this, some approaches employ tagging Magnetic Resonance Imaging (tMRI) [4, 5]. tMRI uses spatial modulation of magnetisation (SPAMM) [5] to visualise the tissue deformation during the cardiac cycle by imprinting a *tagging* pattern in the tissue, see Fig. 1. The method that we present here is based on local frequency estimation and therefore insensitive to tag fading due to spin-lattice relaxation.

Different motion extraction methods have been developed to quantify cardiac function from tMRI. Harmonic Phase (HARP) [6, 7] tracks material points based on the phase conservation principle and is the de facto standard for calculation of cardiac deformation. Other approaches are based on *local frequency* estimation, e.g. [8, 9]. We pursue a new approach, but similar in spirit, in which the Gabor transform is employed to construct a local frequency representation of the tagging images. Subsequently, local frequency covector fields are extracted and used to determine the deformation tensor.

Since our method exploits frequency instead of amplitude information, it is more robust with respect to tag fading. Moreover, the method is designed to work with any number A of tag directions ($A \geq n$, where n denotes spatial dimension), which results in an overdetermined system of equations when $A > n$.

Thus, similarly to Qian et al [8], we bypass the classic approach to assess strain through the gradient of the motion field [10]. In [8], line elements are considered, along which the deformation gradient is calculated and from which linearised radial and circumferential strains are obtained. These are thus confounded with shear strains. However, coordinate independence requires specification of the full strain tensor, which is the approach we choose here. The full deformation tensor thus obtained is used to disentangle radial, circumferential and shear components using the Lagrangian strain tensor. The first two are widely used measures for deformation. In this study, myocardial deformation is assessed using stripe tags in $A \in \{2, 4\}$ directions and grid tags, see Fig. 1.

2 Calculating Deformation from Local Frequency

Let us consider the tissue configuration at two distinct moments of time $t_0 = 0$ and $t > 0$. In an infinitesimally small neighbourhood, the global tagging pattern at time 0 can be considered as a constant frequency pattern $\boldsymbol{\omega}_0$. At time t this frequency pattern is deformed relative to the reference tissue configuration. The Gabor transform [11] offers a position-frequency representation of an image. In the continuous case this Gabor transform reads

$$G(\mathbf{p}, \boldsymbol{\omega}) = \int_{\mathbb{R}^2} f(\mathbf{q})\overline{\psi(\mathbf{q}-\mathbf{p})}\mathrm{e}^{-2\pi\mathrm{i}(\mathbf{q}-\mathbf{p})\cdot\boldsymbol{\omega}}\mathrm{d}\mathbf{q}, \tag{1}$$

where $f : \mathbb{R}^2 \to \mathbb{R}$ is the 2-dimensional tagging image, $\psi : \mathbb{R}^2 \to \mathbb{C}$ the Gabor window, $\bar{\cdot}$ denotes complex conjugation and $\mathbf{p}, \boldsymbol{\omega} \in \mathbb{R}^2$ are position and spatial frequency respectively. For our purpose, we extract a single frequency covector $\boldsymbol{\omega}(\mathbf{p}(t), t)$ at each position $\mathbf{p}(t) = (x(t), y(t))$ at time frame t for each tag direction. A Gaussian window is chosen for ψ, for this has the best position-frequency localisation [12]. Details on the frequency selection method based on the Gabor transform can be found in [13].

While HARP and optical flow assume phase conservation of a material point, this method employs phase difference constancy between tip and tail of a material vector inducing the covector transformation law

$$\boldsymbol{\omega}_t = \boldsymbol{\omega}_0 \mathbf{F}^{-1}, \tag{2}$$

where $\mathbf{F}$ is the deformation tensor [14] and row vectors $\boldsymbol{\omega}_0$, $\boldsymbol{\omega}_t$ represent the local frequencies evaluated at corresponding material points. For more details see [15].

The relation between corresponding material points is not known, since we do not compute material motion. Hence, we assume that at the fiducial moment $t_0 = 0$, when the tagging pattern is applied in the scanner, tag frequency is a known, global constant and therefore equal for every material point, obviating knowledge of material motion. We use this (unobserved) configuration at time $t_0 = 0$ as a reference.

Because a tMRI acquisition typically consists of at least two encoding directions, $A \geq 2$, Eq. (2) constitutes a system of equations that can be written as

$$\boldsymbol{\Omega}_t = \boldsymbol{\Omega}_0 \, \mathbf{F}^{-1}, \text{ with } \boldsymbol{\Omega} = \begin{bmatrix} \boldsymbol{\omega}^1 \\ \vdots \\ \boldsymbol{\omega}^A \end{bmatrix}, \tag{3}$$

with upper indices $1, \ldots, A$ enumerating tag directions. The least squares solution for the deformation tensor at a material point at time t relative to $t_0 = 0$ can then be obtained via the pseudo-inverse

$$\mathbf{F} = \left(\boldsymbol{\Omega}_t^{\mathrm{T}} \boldsymbol{\Omega}_t\right)^{-1} \boldsymbol{\Omega}_t^{\mathrm{T}} \boldsymbol{\Omega}_0, \tag{4}$$

where T denotes transposed. The Lagrangian strain tensor is consequently defined as

$$\mathbf{E} = \frac{1}{2}(\mathbf{F}^{\mathrm{T}}\mathbf{F} - \mathbf{I}). \tag{5}$$

One can extract circumferential (E_{cc}), radial (E_{rr}) and shear (E_{cr}) strains

$$E_{cc} = \hat{\mathbf{e}}_c^{\mathrm{T}}\,\mathbf{E}\,\hat{\mathbf{e}}_c\ ,\ E_{rr} = \hat{\mathbf{e}}_r^{\mathrm{T}}\,\mathbf{E}\,\hat{\mathbf{e}}_r\ ,\ E_{cr} = \hat{\mathbf{e}}_c^{\mathrm{T}}\,\mathbf{E}\,\hat{\mathbf{e}}_r \tag{6}$$

with local unit radial and circumferential basis vectors $\hat{\mathbf{e}}_r$ and $\hat{\mathbf{e}}_c$.

The numerical implementation consists of the following steps:

1. Calculate the Gabor transform $G(\mathbf{p}(t), \boldsymbol{\omega}(t))$ in each pixel, Eq. (1), for all tag directions, using a Gaussian filter ψ with width σ.
2. Determine the local frequency $\boldsymbol{\omega}$ with highest intensity in the Gabor domain, excluding a priori unreachable areas limited by physical muscle deformation.
3. Compute the deformation tensor $\mathbf{F}$, Eq. (4) for every time t, relative to the reference time $t_0 = 0$.
4. Calculate the strain tensor $\mathbf{E}$, Eq. (5), and components E_{rr}, E_{cc} and E_{cr}, Eq. (6).

Here we used $\sigma = 4$. The optimal value of σ depends on the tag width.

3 Data description

In this study, artificial, volunteer and patient tMRI data are used. The artificial tMRI data consisted of a series of 16 frames (64×64 pixels) of contracting and rotating rings, simulating the systolic phase in a single short-axis slice of the left-ventricle, with two and four tag directions ($A \in \{2, 4\}$). The wall thickens and rotation decreases linearly with increasing radius, causing the endocardium to rotate more than the epicardium, inducing shear deformation. Tag fading was modelled by exponential decay and Rician noise was added.

For six volunteers, single short-axis slices of the left-ventricle were obtained in 30 frames with SPAMM imaging, forming a whole heart cycle (systole and diastole). Data was acquired for four tag directions ($A = 4$) with a tag size of 7 mm. Volunteers were scanned with 3T MRI (Achieva, Philips Medical Systems, Best, The Netherlands) after informed consent and with permission given by the Medical Ethical Committee of the local institute.

A 2D multi-shot gradient-echo with Echo Planar Imaging with breath holding in end-expiration was used. Scan parameters were: TE 3.2 ms, TR 6.3 ms, flip angle 10°, slice thickness 10 mm and acquisition pixel size 1.34×1.34 mm^2 for volunteer 2 and 1.37×1.37 mm^2 for all other volunteers. Prospective triggering was used with a maximal number of reconstructed phases to ensure optimal temporal resolution. Contours of the myocardium were manually drawn.

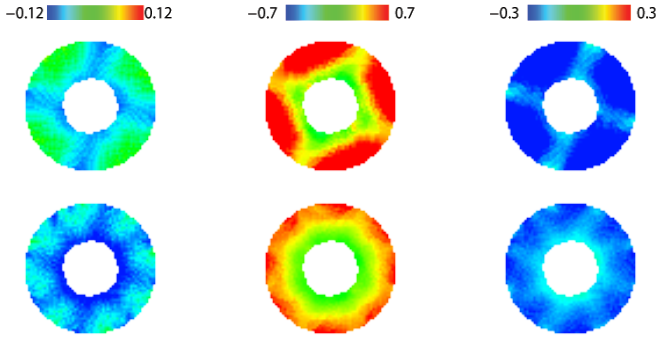

Fig. 2. Short-axis view of circumferential (left), radial (middle), and shear (right) components of the Lagrangian strain tensor for artificial data (mid-systole) comparing two diagonal (top) with four (bottom) tag directions.

Table 1. Average displacement errors of a rectangular grid for two and four tag directions using our novel method and HARP in mid-systole on artificial tMRI data.

	hor. and vert. directions	diagonal directions	four directions
Gabor estimation	0.5 ± 0.22 px	0.38 ± 0.2 px	0.32 ± 0.14 px
HARP	0.54 ± 0.07 px	0.54 ± 0.05 px	0.53 ± 0.07 px

The patient dataset was obtained with a 2D SPAMM gradient-echo sequence with breath holding in end-expiration. Scan parameters were: 1.5T MRI, TE 4 ms, TR 6.4 ms, a tag size of 7 mm, slice thickness 8 mm and acquisition pixel size 1.33×1.33 mm^2.

4 Results

For both artificial and volunteer data, local frequencies were calculated for all tag directions. We tested our method for both two ($A=2$) and four ($A=4$) tag directions. An adapted implementation was used for the grid tagging sequence of the patient dataset. In this case, two dominant peaks were located in the Gabor domain to determine the local frequencies corresponding to the two tag orientations of the grid. For all datasets, deformation tensors were computed according to Eq. (4). These were used to obtain radial, circumferential and shear strains, as presented in Fig. 2, Fig. 3 and Fig. 4.

For the artificial data, based on the deformation tensors from Eq. (4) displacements were calculated for a large number of points organized in a rectangular grid. The results of our method as well as deformed lattices calculated by our own implementation of HARP [16] are compared with the ground truth, using both four and two tag directions as inputs. We adapted HARP to accept four input image sequences by adding two equations to the iterative scheme and solving the obtained system with the least squares method. Although more precise implementations of HARP exist, we chose to use the faster implementation based

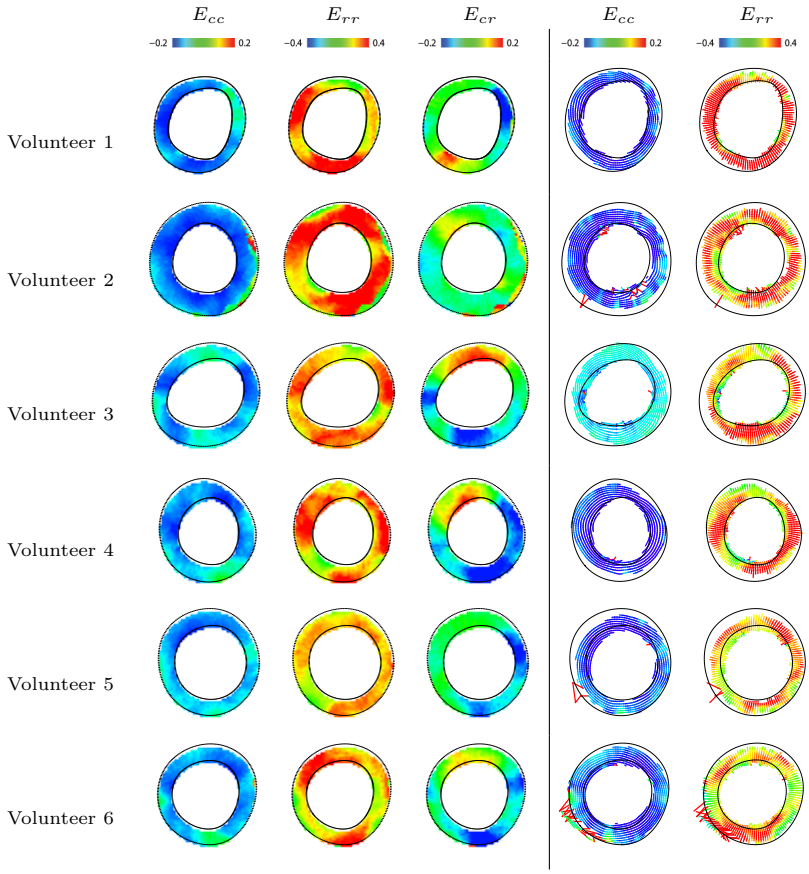

Fig. 3. Strain computed in short-axis view of the left ventricle (volunteer) for four tag directions. Left: Components of the Lagrangian strain tensor in end systole obtained with local frequency extraction. Right: Linearised strains obtained with HARP.

on linearised strains [6]. As a consequence, these linearised strains can not be directly compared with strain results of our method. Therefore, Table 1 shows the average displacement errors in pixels with respect to their true counterparts (average distance between calculated and true grids) in the mid-systolic frame using our novel method and HARP.

5 Discussion and Conclusion

We have shown that quantitative myocardial deformation can be accurately and robustly obtained from the Gabor frequency analysis of artificial tMRI data using four tag directions. Our method does neither require explicit knowledge of material motion nor tag line extraction. It is robust with respect to tag fading and can be straightforwardly generalised to any number of tag directions and

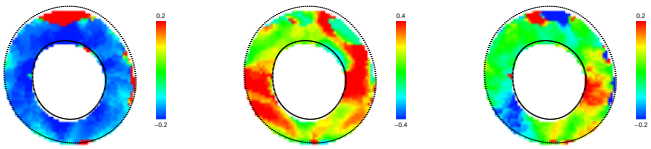

Fig. 4. Short-axis view of left ventricle *grid tagging* slice in end-systole (patient). Circumferential, radial, and shear components of the Lagrangian strain tensor respectively.

to volumetric tagging data. Moreover, the proposed method uses the full form of the strain tensor instead of approximated linearised strain, which is used for HARP strain calculations. Due to the fact that estimated frequencies are directly used to calculate deformations, the smoothness of the frequency map has a major influence on the results. This effect is expected to be reduced by means of adapting the Gabor filter depending on the location in the muscle or muscle width, cf. [13], which is a subject for future work. Position dependent weighting in the least squares method Eq. (4) may lead to additional improvements. Nevertheless, subsequent approximation of tissue displacements performs comparably to HARP, while unlike with HARP using four tag directions improves the quality of the results in comparison with using two tag directions (cf. Table 1). Since HARP is an iterative method, it stops after a certain prescribed tolerance is achieved. This explains why the performance of HARP does not improve with more tag directions. Interestingly, and somewhat unexpectedly, a combination of diagonal tag patterns performs better than a horizontal-vertical tag pattern in artificial data. Considering the approximate rotational symmetry of the model, this is most likely caused by a discretisation effect related to the relative orientations of tag lines and pixel grid.

In contemporary medical practice it is common to use only two tag directions for analysis. We used more directions to achieve more stable and homogeneous results, which may increase acquisition time. However, this can be prevented by using one or two grid patterns consisting of multiple, simultaneously acquired tag directions. Applicability of our method to a diagonal grid tagging sequence is shown on clinical data. Combining horizontal, vertical and diagonal tagging stripes in two grids will preserve robustness and keep acquisition times clinically acceptable.

Acknowledgements The authors would like to thank dr. Brett Cowan and dr. Alistair Young, University of Auckland, New Zealand for providing the patient data set.

References

1. Götte, M.J., van Rossum, A.C., Twisk, J.W.R., Kuijer, J.P.A., Marcus, J.M., Visser, C.A.: Quantification of regional contractile function after infarction: Strain analysis superior to wall thickening analysis in discriminating infarct from remote myocardium. Journal of the American College of Cardiology **37** (2001) 808–817

2. Delhaas, T., Kotte, J., van der Toorn, A., Snoep, G., Prinzen, F.W., Arts, T.: Increase in left ventricular torsion-to-shortening ratio in children with valvular aorta stenosis. Magnetic Resonance in Medicine **51** (2004) 135–139
3. Bohs, L., Geiman, B., Anderson, M., Gebhart, S., Trahey, G.: Speckle tracking for multi-dimensional flow estimation. Ultrasonics **38** (2000) 369375
4. Zerhouni, E.A., Parish, D.M., Rogers, W.J., Yang, A., Shapiro, E.P.: Human heart: Tagging with MR imaging—a method for noninvasive assessment of myocardial motion. Radiology **169**(1) (1988) 59–63
5. Axel, L., Dougherty, L.: MR imaging of motion with spatial modulation of magnetization. Radiology **171**(3) (1989) 841–845
6. Osman, N.F., Kerwin, W.S., McVeigh, E.R., Prince, J.L.: Cardiac motion tracking using CINE harmonic phase (HARP) magnetic resonance imaging. Magnetic Resonance in Medicine **42**(6) (1999) 1048–1060
7. Garot, J., Bluemke, D.A., Osman, N.F., Rochitte, C.E., McVeigh, E.R., Zerhouni, E.A., Prince, J.L., Lima, J.A.C.: Fast determination of regional myocardial strain fields from tagged cardiac images using harmonic phase MRI. Circulation **101**(9) (March 2000) 981–988
8. Qian, Z., Liu, Q., Metaxas, D., L., A.: Identifying regional cardiac abnormalities from myocardial strains using non-tracking-based strain estimation and spatio-temporal tensor analysis. IEEE Transactions on Medical Imaging **30**(12) (2011) 2017 – 2029
9. Arts, T., Prinzen, F.W., Delhaas, T., Milles, J.R., Rossi, A.C., Clarysse, P.: Mapping displacement and deformation of the heart with local sine-wave modeling. IEEE Transactions on Medical Imaging **29**(5) (May 2010)
10. Florack, L., van Assen, H.: A new methodology for multiscale myocardial deformation and strain analysis based on tagging MRI. International Journal of Biomedical Imaging (2010) http://dx.doi.org/10.1155/2010/341242.
11. Gabor, D.: Theory of communication. part 1: The analysis of information. Journal of the Institution of Electrical Engineers - Part III: Radio and Communication Engineering **93**(26) (november 1946) 429–441
12. Mallat, S.: A wavelet tour of signal processing. Academic Press (1999)
13. Duits, R., Führ, H., Janssen, B., Bruurmijn, M., Florack, L., van Assen, H.: Evolution equations on Gabor transforms and their applications. Applied and Computational Harmonic Analysis (2012) http://dx.doi.org/10.1016/j.acha.2012.11.007.
14. Haupt, P.: Continuum Mechanics and Theory of Materials. Springer-Verlag, Berlin (2002)
15. Bruurmijn, L., Kause, H., Filatova, O., Duits, R., Fuster, A., Florack, L., van Assen, H.: Myocardial deformation from local frequency estimation in tagging mri. In Ourselin, S., Rueckert, D., Smith, N., eds.: Functional Imaging and Modeling of the Heart. Volume 7945 of Lecture Notes in Computer Science., Heidelberg, Springer (2013) 284–291
16. Osman, N.F., McVeigh, E.R., Prince, J.L.: Imaging heart motion using harmonic phase MRI. IEEE Transactions on Medical Imaging **19**(3) (2000) 186–202